Gate-controlled Ambipolar Transport in b-AsP Crystal and Its VIS-NIF Photodetection

Mianzeng Zhong,[a] Haotong Meng,[a] Zhihui Ren,[b] Le Huang,[c] Juehan Yang,[b] Bo Li,[d] Qinglin Xia,[a] Xiaoting Wang,[b] Zhongming Wei,[b] Jun He,*[a]

[a]*Hunan Key Laboratory of Nanophotonics and Devices, School of Physics and Electronics, Central South University, Changsha 410083, Hunan, China. E-mail: junhe@csu.edu.cn*

[b]*State Key Laboratory of Superlattices and Microstructures, Institute of Semiconductors, Chinese Academy of Sciences & Center of Materials Science and Optoelectronics Engineering, University of Chinese Academy of Sciences, Beijing 100083, China. E-mail: xiaoting13@semi.ac.cn*

[c]*School of Materials and Energy, Guangdong University of Technology, Guangzhou 510006, China*

[d]*Department of Applied Physics, School of Physics and Electronics, Hunan University, Changsha 410082, Hunan, China*

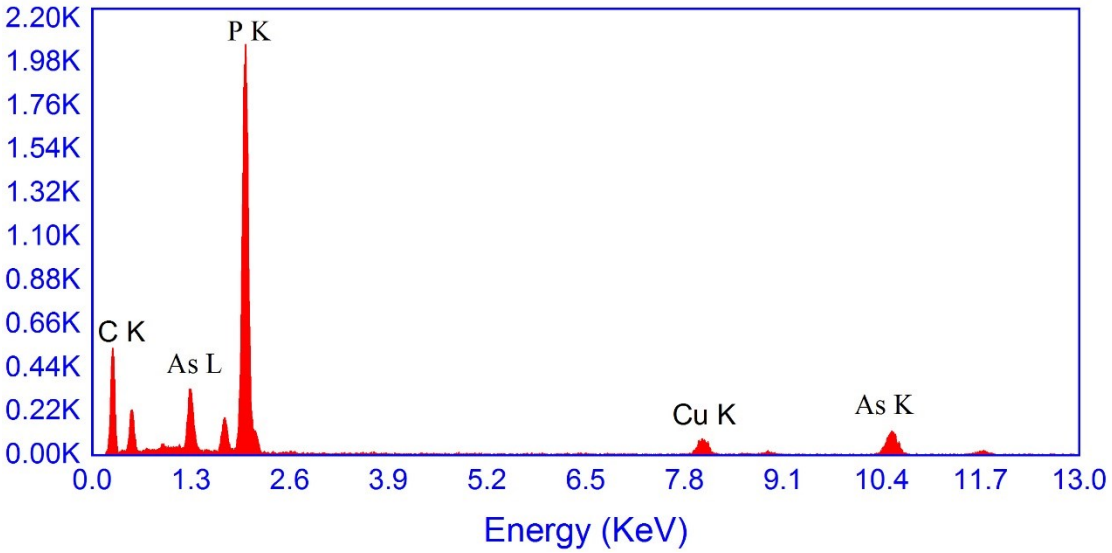

Figure S1. The representative EDX spectrum of the b-$As_{0.084}P_{0.916}$ crystal. The Cu and C signals come from the copper grid.

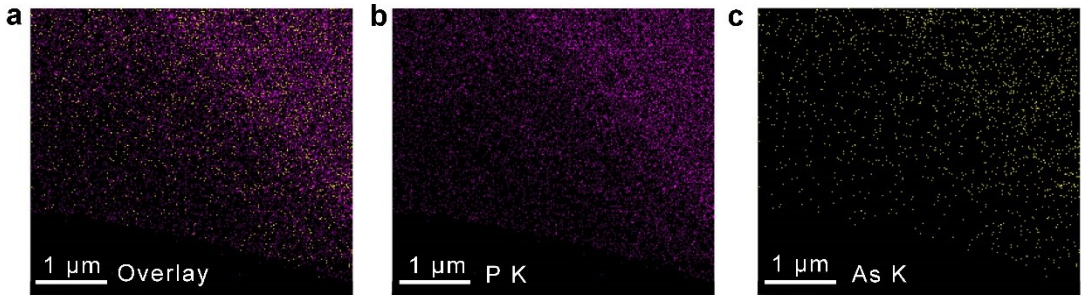

Figure S2. HAADF STEM-EDX mappings of a typical b-$As_{0.084}P_{0.916}$ nanoflake reveal uniform elemental distributions.

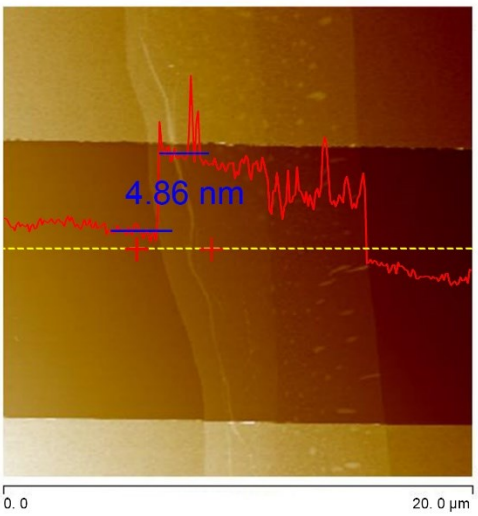

Figure S3. AFM image of a typical b-$As_{0.084}P_{0.916}$ based FET, the thickness is 4.86 nm.

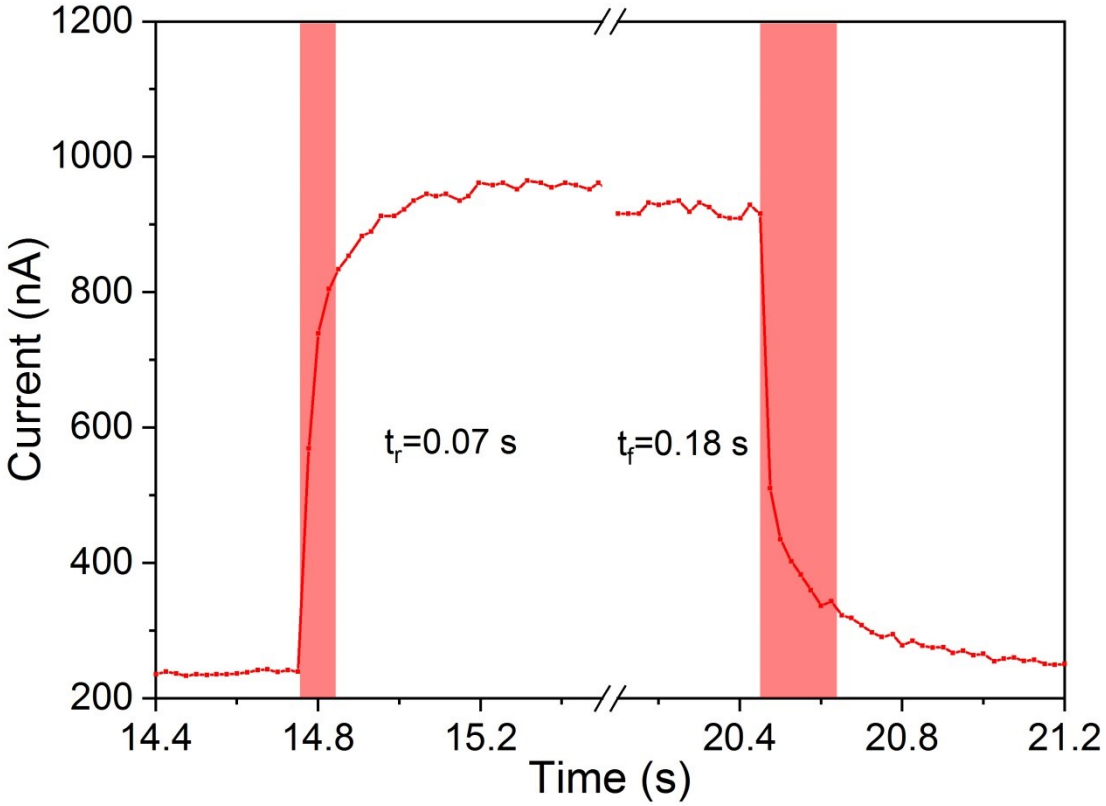

Figure S4. Photocurrent rise and decay time of this device measured at a bias voltage of 1 V and under illumination of 638 nm laser with a light intensity of 73 mW/cm^2.

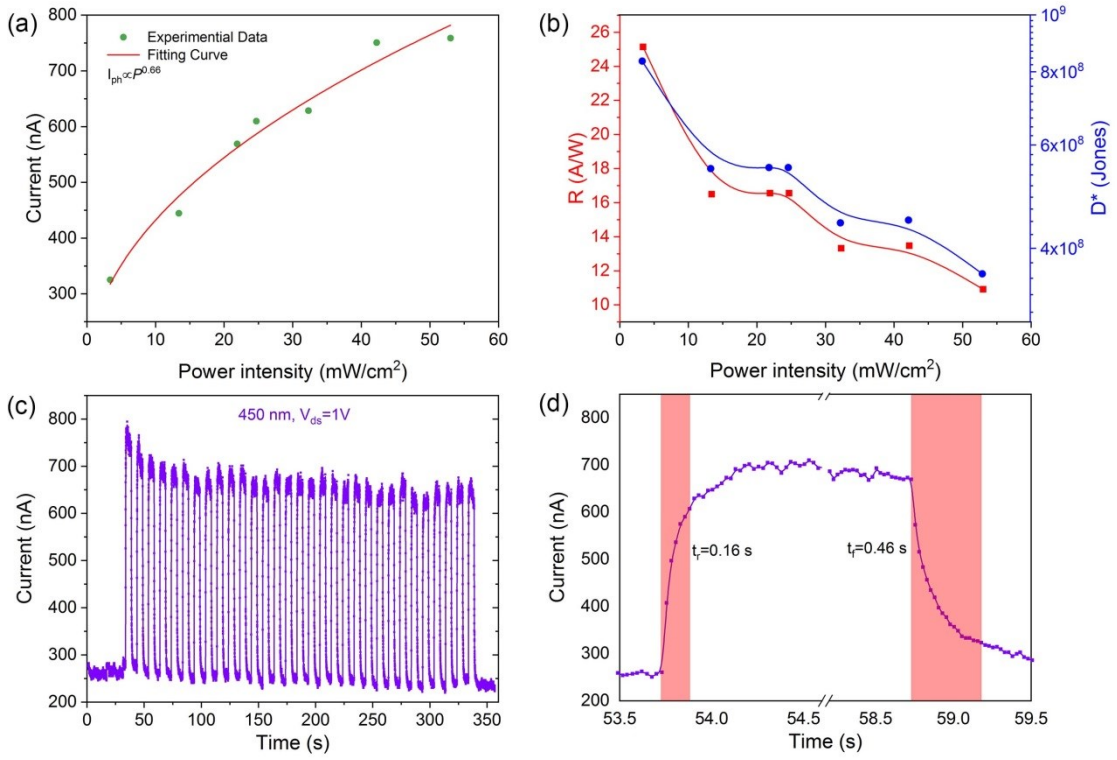

Figure S5. (a) The light power intensity dependence of the photocurrent measured with a bias voltage of 1 V under the illumination of 450nm laser; (c) Light intensity dependent responsivity and detectivity at the illumination of 450 nm laser under a bias of 1 V; (d) The photoswitching behaviour, (e) photocurrent rise and decay time of this device under illumination of 450 nm laser with a light intensity of 53 mW/cm^2 and a bias voltage of 1 V.

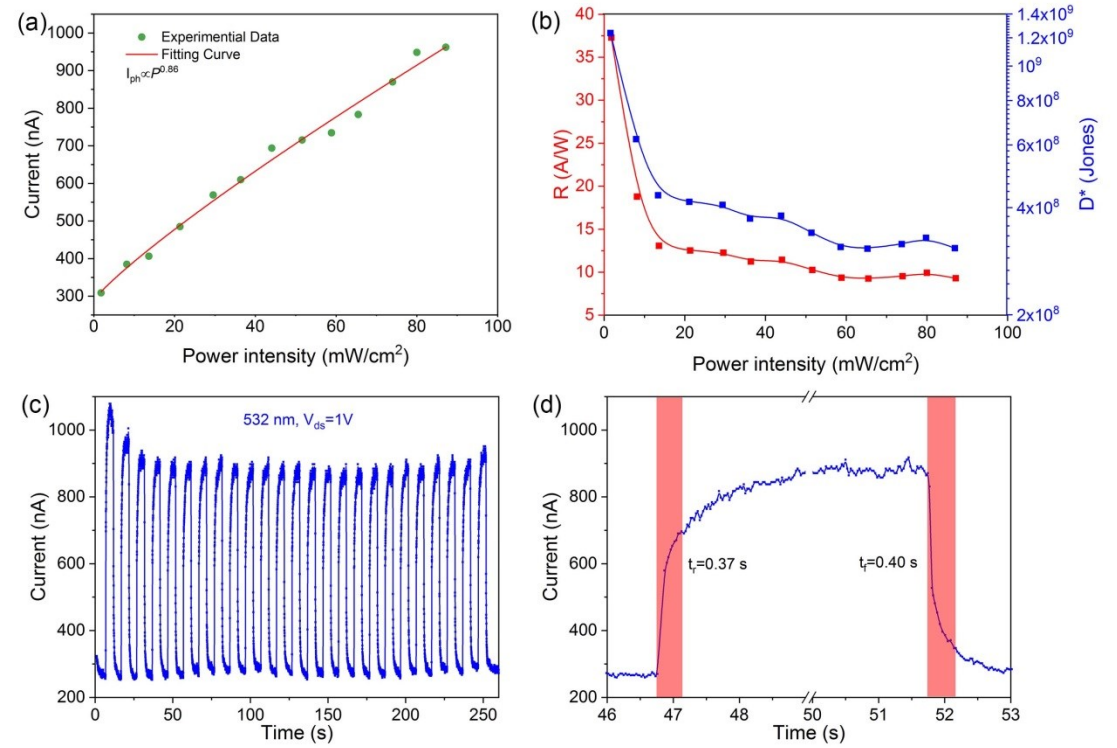

Figure S6. (a) The light power intensity dependence of the photocurrent measured with a bias voltage of 1 V under the illumination of 532nm laser; (c) Light intensity dependent responsivity and detectivity at the illumination of 532 nm laser under a bias of 1 V; (d) The photoswitching behaviour, (e) photocurrent rise and decay time of this device under illumination of 532 nm laser with a light intensity of 88 mW/cm^2 and a bias voltage of 1 V.

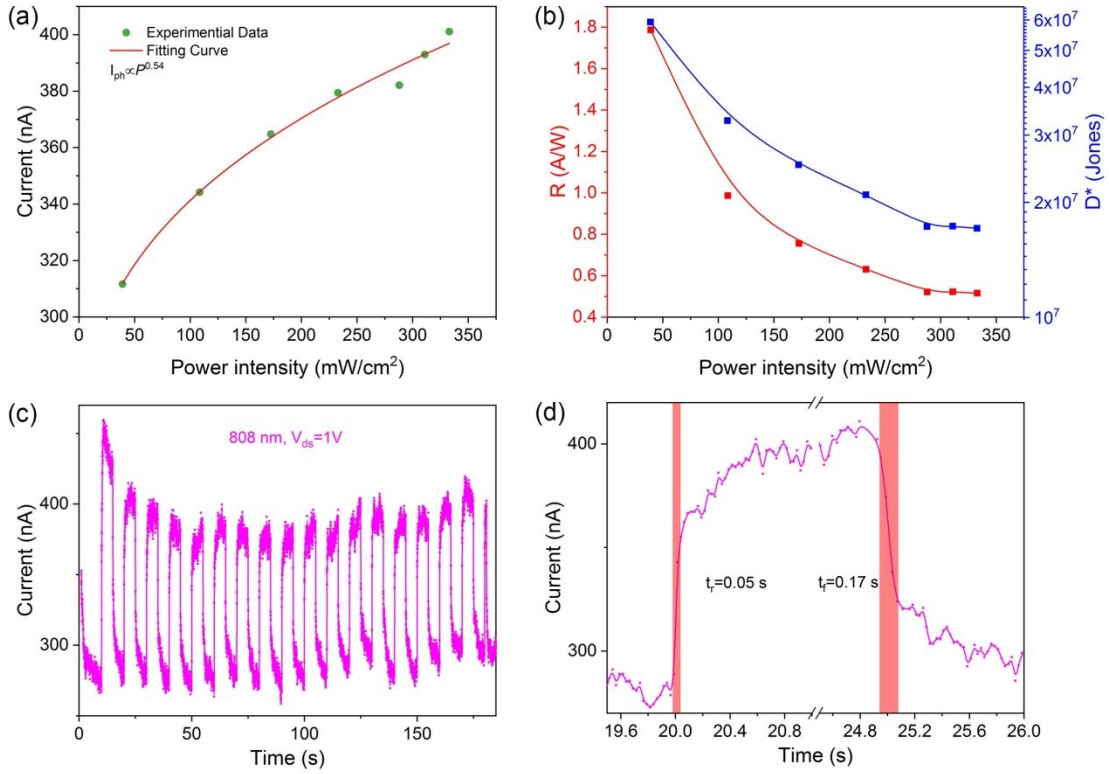

Figure S7. (a) The light power intensity dependence of the photocurrent measured with a bias voltage of 1 V under the illumination of 808nm laser; (c) Light intensity dependent responsivity and detectivity at the illumination of 808 nm laser under a bias of 1 V; (d) The photoswitching behaviour, (e) photocurrent rise and decay time of this device under illumination of 808 nm laser with a light intensity of 328 mW/cm^2 and a bias voltage of 1 V.

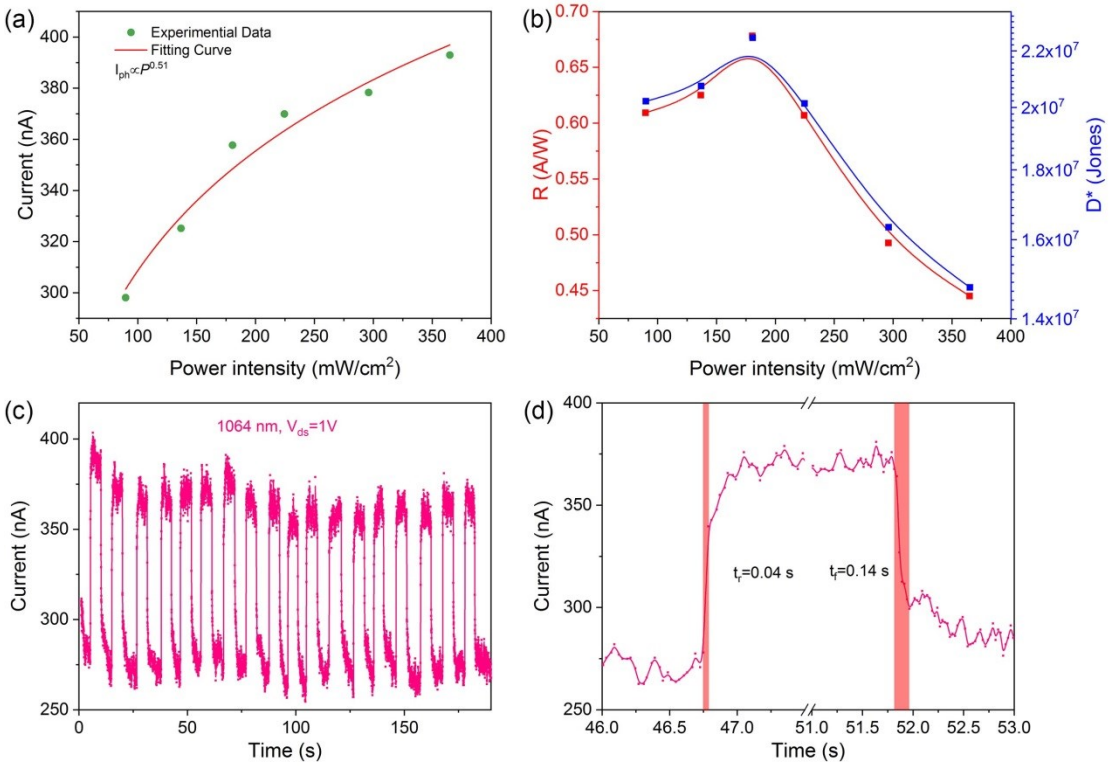

Figure S8. (a) The light power intensity dependence of the photocurrent measured with a bias voltage of 1 V under the illumination of 1064 nm laser; (c) Light intensity dependent responsivity and detectivity at the illumination of 1064 nm laser under a bias of 1 V; (d) The photoswitching behaviour, (e) photocurrent rise and decay time of this device under illumination of 1064 nm laser with a light intensity of 368 mW/cm^2 and a bias voltage of 1 V.

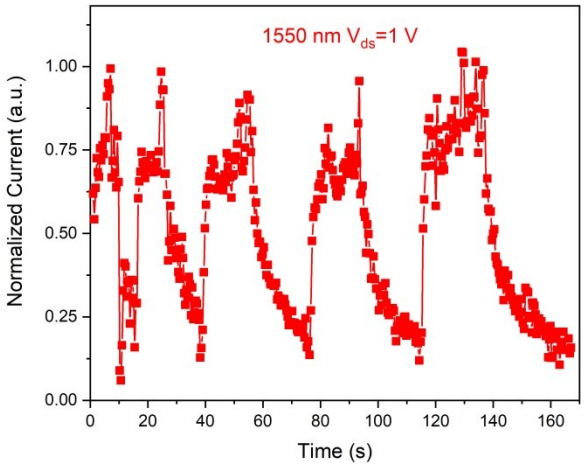

Figure S9 (a) The photoswitching behaviour of a typical device under illumination of 1550 nm with the light intensity of 72.2 mW/cm^2.